Noncoherent Eigenbeamforming and Interference Suppression for Outdoor OFDM Systems

Noah Jacobsen, *Member, IEEE*, Gwen Barriac, *Member, IEEE*, and Upamanyu Madhow, *Fellow, IEEE*

***Abstract*—We investigate a new approach to uplink communications in wideband outdoor cellular systems that can take advantage of multiple antennas at the base station in a scalable manner, while eliminating or minimizing overhead for channel estimation. The proposed techniques, which focus on exploiting correlated channels with the use of closely spaced antenna arrays, are applicable to emerging Orthogonal Frequency Division Multiplexing (OFDM) based Wireless Metropolitan Area Network (WMAN) systems, such as those based on the IEEE 802.16/20 standards. Outdoor channels frequently have a small number of dominant spatial modes, which can be learned from overhead-free estimation of the spatial covariance matrix by averaging across subcarriers. We describe an *eigenbeamforming* receiver which projects the received signal along the dominant spatial modes, yielding a beamforming gain that scales up with the number of receive elements and a diversity level depending on the number of dominant spatial modes. Shannon limits are first computed for block fading approximations to time- and frequency-selective channels. The suboptimal noncoherent diversity-combining receiver is shown to approach these limits, with linear complexity in the number dominant modes. Further, for dealing with spatially non-white interfering signals, adaptive suppression techniques are shown to mitigate strong interference with minimal training overhead.**

***Index Terms*—Multi-Input Multi-Output (MIMO) noncoherent communication, beamforming, Orthogonal Frequency Division Multiplexing (OFDM), Quadrature Amplitude Modulation (QAM), Error Correcting Codes (ECC), interference suppression.**

I. Introduction

THIS paper is motivated by the following question: how can we best use multiple antennas at the base station of a wideband wireless system supporting high data rates and mobility, when the subscriber unit (or mobile) is limited to a small number of antennas (e.g., one or two)? We focus on OFDM, which is the modulation strategy of choice for emerging WMAN standards based on IEEE 802.16 and 802.20. Our prior work [1] focused on optimizing the downlink of such systems, exploiting the specific features of outdoor channels and the asymmetry in capabilities of the base station and the subscriber unit. In this paper, we investigate uplink transceiver design. We wish to obtain designs which scale up in performance as the number of base station antennas increases, without significantly increasing signal processing complexity or channel estimation overhead.

When the (base station) receiver has an antenna array, the optimal strategy in a coherent OFDM system is to perform maximal ratio combining, or receive beamforming, which requires knowledge of the array response. We focus on channels that exhibit fast variations in time due to mobility, and in frequency due to large delay spreads. Thus, estimation of the array response for each subcarrier, as required for coherent receive beamforming, involves significant overhead for channel estimation. In this paper, we specifically consider channels with a few number of dominant spatial modes, as are common in outdoor cellular applications where the base station is generally elevated above the mobiles. For such channels, we propose noncoherent communication techniques that use closely-spaced arrays to obtain beamforming gains and interference suppression while eliminating or significantly reducing channel overhead.

We assume that the base station has N antenna elements and the mobile has one antenna; although the concepts are generalizable to multi-antenna transmissions. The design is based on the following observations regarding outdoor spatial channels: First, the space-time channel for each subcarrier can be modeled as identically distributed complex Gaussian random vectors that decorrelate across frequency [2]. This implies that we can estimate the distribution of these vectors by simply estimating the spatial channel covariance matrix, averaged across subcarriers. Second, for elevated base stations, there is little scattering around the base station, so that the incoming signal from a given mobile has a narrow Power Angle Profile (PAP). This implies that the spatial covariance matrix has a small number of dominant eigenmodes (typically one, two, or three), even as we scale up the number of base station antennas. Thus, most of the received signal energy can be captured by projecting along the dominant eigenmodes. Finally, while the channel realization in each subcarrier can vary rapidly with time due to fading, the spatial covariance matrix varies much more slowly, since it depends only on the coarse system geometry.

These observations motivate the proposed *noncoherent eigenbeamforming* receiver. The dominant eigenmodes are estimated from the received signal by averaging the empirical spatial covariance (across time and/or frequency). The received signal is projected along the dominant modes. That is, we

Paper approved by J. Wang, the Editor for Wireless Spread Spectrum of the IEEE Communications Society. Manuscript received May 1, 2006; revised January 29, 2007 and July 12, 2007.

N. Jacobsen is with Alcatel-Lucent, Murray Hill, NJ 07974 USA (e-mail: jacobsen@alcatel-lucent.com). This work was performed while with the Dept. of Electrical and Computer Engineering, University of California, Santa Barbara, CA 93106.

G. Barriac is with Qualcomm, Inc., San Diego, CA 92121 (e-mail: gbarriac@qualcomm.com). This work was performed while with the Dept. of Electrical and Computer Engineering, University of California, Santa Barbara, CA 93106.

U. Madhow is with the Dept. of Electrical and Computer Engineering, University of California, Santa Barbara, CA 93106 (e-mail: madhow@ece.ucsb.edu).

Digital Object Identifier 10.1109/TCOMM.2008.060269.

employ a small number (namely L) of fixed beamformers for the entire wideband signal, rather than using separate beamformers for each subcarrier. This provides a "beamforming gain" of roughly N/L and a "diversity level," or degree of spatial parallelization, of roughly L, where these terms are defined more precisely later. We now obtain L scalar OFDM channels in parallel. For each of these, turbo-like noncoherent joint data and channel estimation is employed, as in prior work on single antenna channels [3], [4], [5], with a fading model that approximates the complex channel gain as constant over a block of symbols spanning both time and frequency. The size of the *coherence block* is chosen inversely proportional to the Doppler frequency times the delay spread. Thus, use of a block fading model is consistent with the assumption of mobility and frequency-selectivity by appropriate choice of the block size and with an appropriate mapping of the transmitted symbols to time and frequency bins. A coherence block size of ten symbols is used in the performance evaluations. We provide capacity results for an L-fold block fading model and show that suboptimally combining the outputs from L parallel noncoherent demodulators is effective in terms of approaching the capacity.

The assumption of overhead-free spatial covariance information holds true for all channels with a non-zero delay spread in the wideband limit. For example, in a 20 MHz system, delay spreads on the order of hundreds of nano-seconds yield channels with sufficient level of frequency diversity. Moreover, since the spatial modes evolve continuously in time, temporal averaging can further be obtained, which depends on the velocity. An important consequence is that the antenna elements are to be closely spaced in order to resolve the spatial correlations. We show that, for such channels, multi-antenna noncoherent techniques are able to provide comparable performance to Shannon limits with a reasonable level of complexity, thereby saving any channel estimation overhead that is otherwise required.

While the preceding receiver requires no pilot overhead for channel estimation, it does not account for spatially colored interference, which might arise, for example, due to simultaneous transmissions in nearby cells or sectors. In this case, the covariance matrix may contain dominant spatial modes due to both the desired signal and the interference. We propose linear Minimum Mean Squared Error (MMSE) based interference suppression techniques compatible with noncoherent demodulation, using pilots from the desired user for training. Specifically, we adapt the Differential MMSE (DMMSE) criterion, developed for direct sequence systems with fading channels [6], to obtain an interference suppression technique that is robust to channel variations across time and frequency. The interference suppression correlators are applicable to the entire wideband signal, and are followed up by turbo-like noncoherent processing.

Related work: Transceiver designs for space-time communication have traditionally addressed narrowband channels in rich scattering environments typical of indoor channels. In a seminal work of Telatar [7], it is shown that such channels exhibit a linear scaling (in the minimum of the number of transmit and receive elements) in capacity when the channel is known to transmitter and receiver. Constructive space-time coding techniques have been developed, for example [8], [9], [10], which are able to realize the advantage of having multiple antennas in a coherent system. In contrast to these works, we consider wideband, frequency-selective fading channels for which the assumption of perfect channel knowledge is not practical. Moreover, the outdoor environments modeled here commonly give rise to channels with a high degree of spatial correlation.

Marzetta and Hochwald first characterized the *noncoherent capacity* of a multi-antenna isotropic block fading channel [11]. A geometric approach for characterizing the noncoherent capacity, which generalizes geometric interpretations for classical coherent channels, is developed in [12]. Here we consider spatially correlated channels, employing block fading to model time-frequency coherence. In [13], the capacity with QPSK signals of L parallel block fading channels is quantified. Such computations reveal a modest gain of up to 2 dB at mid-to-high Signal-to-Noise Ratio (SNR) for channels with equal strength dominant spatial modes. Low SNR channels do not exhibit any diversity advantage.

A turbo architecture for noncoherent communication over single-antenna block fading channels is developed in [4]. The proposed noncoherent eigenbeamforming receiver leverages spatial covariance information inherent to wideband signals for processing the multiple spatial modes of the received signal. Constructive coding techniques for MIMO noncoherent communication have also been proposed in [14], [15]. Here we emphasize the complexity advantages of noncoherent eigenbeamforming, while maintaining near capacity performance. The concept of diversity combining with multiple noncoherent eigenmodes is also considered in [6], where an *eigen-rake* receiver for Code Division Multiple Access (CDMA) systems with multi-path interference is introduced.

Map of paper: We begin by providing numerical examples of beamforming gains typical of urban cellular channels in Section II. The examples show that for such channels the received signal strength plateaus quickly with the number of dominant modes employed at the receiver. In Section III, the performance of noncoherent eigenbeamforming is evaluated with a constructive coded modulation scheme consisting of a convolutional code serially concatenated with differential QPSK. For multiple dominant eigenmodes, optimal noncoherent processing is too complex and our numerical results compare performance of suboptimal noncoherent diversity combining with the information-theoretic benchmarks we have obtained.

The DMMSE framework for interference suppression is developed and evaluated in Section IV. The simulation results confirm that relatively few pilots, approximately 2%, are required to train DMMSE correlators to the dominant spatial modes of the desired signal. Thus, when the dominant modes of the signal and interference channels are roughly orthogonal, which is likely to occur, for example, when the mean angle of arrival for the two channels is separated by 45°, performance approaches that with no interference.

II. Noncoherent Eigenbeamforming

Accurate estimates of the spatial covariance matrix, available from averaging in wideband systems, allow eigenbeam-

forming at the receiver with the dominant spatial modes of the channel [13]. Much of the Multi-Input Multi-Output (MIMO) communication literature assumes channel coherence (see [16] and the references therein) and classical receive beamforming is based on explicit channel estimations [7]. We demonstrate that beamforming gains are realizable with multi-antenna noncoherent receivers, despite lack of transmitted pilots.

For typical outdoor channels, where the number of dominant spatial modes is small, noncoherent eigenbeamforming is able to increase SNR by scaling up the number of antennas, while limiting demodulation and decoding complexity, which scales with the number of dominant modes. Noncoherent beamforming techniques are well-suited to the uplink of cellular systems, where the base station must track a time-varying channel to each mobile. Pilot-symbol based channel estimates are potentially more efficient on the downlink, where the mobiles are able to share a common pilot channel.

First, material from our earlier work [2], [17], which abstracts simple statistical models from the literature on outdoor channel measurements, is reviewed. We then show that, for typical outdoor channels, most of the beamforming gains relative to a single antenna system can be obtained by using a small number of modes.

Notation: The conjugate transpose of vector $\mathbf{x}$ is written $\mathbf{x}^{\mathrm{H}}$, while $\langle \mathbf{x}, \mathbf{y} \rangle = \mathbf{y}^{\mathrm{H}}\mathbf{x}$ denotes the inner product of vectors $\mathbf{x}$ and $\mathbf{y}$. The $N \times N$ identity matrix is written as I_N. The Kronecker delta function, δ_{jk}, is defined as one for $j = k$ and zero otherwise. The expectation, trace, and determinant operators are denoted: E, tr, and $\det$, respectively.

A. OFDM System Model

As in the classical Saleh-Valenzuela model [18], the channel impulse response is decomposed into clusters (dominant reflecting bodies). Experimental measurements of outdoor channels [19] indicate that the number of clusters is small, usually one or two, and that the Power Delay Profile (PDP) and the Power Angle Profile (PAP) for each cluster can be modeled with exponential and Laplacian densities, respectively.

A mobile with one antenna communicates the OFDM signal with K subcarriers to an N element receive array. The received signal vector on the kth subcarrier is given by

$$\mathbf{y}[k] = \mathbf{h}[k]x[k] + \mathbf{n}[k],$$

where $\mathbf{h}[k]$ is an $N \times 1$ channel frequency response, $\mathbf{n}[k]$ is Additive White Gaussian Noise (AWGN) with $\mathrm{E}(\mathbf{n}[j]\mathbf{n}[k]^{\mathrm{H}}) = 2\sigma^2\delta_{jk}\mathrm{I}_N$. It follows from our earlier work [2] that the $\{\mathbf{h}[k]\}$ are well-modeled as identically distributed zero-mean proper complex Gaussian random vectors,

$$\mathbf{h}[k] \sim \mathcal{CN}(0, \mathrm{C}),$$

with covariance matrix

$$\mathrm{C} = \mathrm{E}\left(\mathbf{a}(\Omega)\mathbf{a}(\Omega)^{\mathrm{H}}\right), \tag{1}$$

where $\mathbf{a}(\Omega) = [a_1(\Omega) \cdots a_N(\Omega)]^{\mathrm{T}}$ denotes the base station array response for angle of arrival Ω. A standard linear array is modeled, for which

$$a_n(\Omega) = \mathrm{E}\left(j(n-1)2\pi\frac{d}{\lambda}\sin(\Omega)\right),$$

where d is the antenna array spacing and λ is the carrier wavelength. We specifically consider closely spaced arrays (or beamforming arrays), with $d = \lambda/2$ unless otherwise indicated. The expectation (1) is taken over the distribution of Ω, the PAP.

A spectral decomposition of the channel covariance yields

$$\mathrm{C} = \mathrm{U}\Lambda\mathrm{U}^{\mathrm{H}} \tag{2}$$

where the eigenvector matrix $\mathrm{U} = [\mathbf{u}_1 \cdots \mathbf{u}_N]$ is unitary, $\mathbf{u}_l$ denotes the lth eigenvector, and Λ is diagonal with eigenvalues $\{\lambda_l\}_{l=1}^N$ arranged in decreasing order. The eigenvalue λ_l represents the energy of the channel along the lth spatial mode $\mathbf{u}_l$.

B. Covariance Estimation

For large delay spreads typical of outdoor environments, the coherence bandwidth is small, and the correlation between the channel responses at different frequencies dies out quickly with their separation. Thus, the base station can accurately estimate the spatial covariance matrix C by measuring the channel over a rich enough set of uplink frequencies [17].

Averaging over frequency bins, the base station forms the empirical autocorrelation matrix:

$$\mathrm{Q} = \frac{1}{K}\sum_{k=1}^{K}\mathbf{y}[k]\mathbf{y}[k]^{\mathrm{H}}.$$

With $\mathrm{E}(|x[k]|^2) = 1$, it is easy to show that Q is an estimate of $\mathrm{C} + 2\sigma^2\mathrm{I}_N$, where σ^2 is the noise variance per dimension. Thus, the lth eigenvalue of Q is given by $\lambda_l + 2\sigma^2$, and the eigenvectors of Q and C are the same.

An eigen-decomposition of Q thus yields the dominant channel eigenmodes. Typically, the number of dominant modes is small for an outdoor channel because of the narrow PAP corresponding to signals received from a given mobile.

C. Eigenbeamforming

We now perform receive beamforming along the principal eigenvectors of Q, namely, $\mathbf{u}_1, \mathbf{u}_2, \cdots, \mathbf{u}_L$. The received vectors in each frequency bin are projected along these eigenvectors to get L scalar OFDM signals, where L is typically much smaller than the number of antenna elements. A receiver block diagram is depicted in Figure 1. The lth symbol at subcarrier k is given by:

$$z_l[k] = \langle \mathbf{u}_l, \mathbf{y}[k] \rangle = \alpha_l[k]x[k] + w_l[k],$$

where $\alpha_l[k] = \langle \mathbf{u}_l, \mathbf{h}[k] \rangle$, $l = 1, \ldots, L$, are independent Gaussian channels, with $\alpha_l[k] \sim \mathcal{CN}(0, \lambda_l)$. The AWGN is given by $w_l[k] = \langle \mathbf{u}_l, \mathbf{n}[k] \rangle$, where $\mathrm{E}(w_l[j]w_m^*[k]) = 2\sigma^2\delta_{jk}\delta_{lm}$.

1) Eigenbeamforming gain: As a rough measure of the performance gain relative to a single antenna system, we define the beamforming gain as the SNR if signal power is summed over the L selected spatial modes, relative to the SNR for a single antenna system. This yields the following formula for the beamforming gain as a function of L:

$$G(L) = \frac{N}{\mathrm{tr}(\mathrm{C})}\sum_{l=1}^{L}\lambda_l. \tag{3}$$

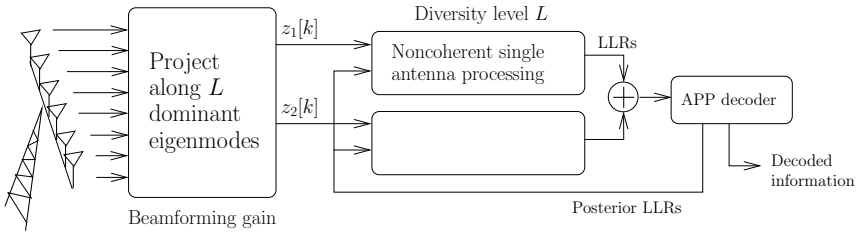

Fig. 1. Noncoherent eigenbeamforming receiver, $L = 2$.

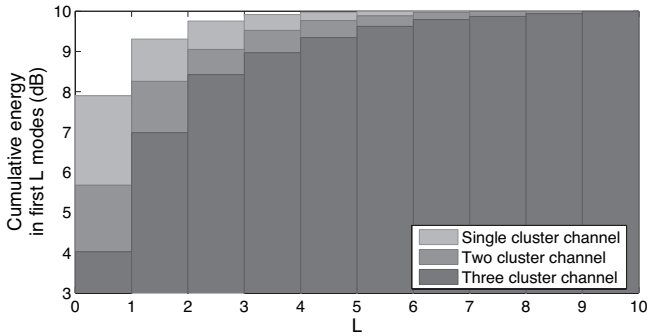

Fig. 2. Eigenbeamforming gain with respect to a single antenna receiver.

Figure 2 shows the beamforming gain in dB as a function of the number of eigenmodes for a 10-antenna linear array with $\lambda/2$ spacing. The upper curve is for a single cluster channel whose PAP is Laplacian, $\Omega \sim \mathcal{L}(\theta, \Delta)$, with mean $\theta = 0°$, and angular spread $\Delta = 10°$. The angular spread of a Laplacian random variable is defined as twice the mean of the corresponding exponential random variable, $|\Omega - \theta|$, as $\Delta = 2\,\mathrm{E}(|\Omega - \theta|)$. The middle plot is for a two cluster channel with the first PAP as above and the second PAP also Laplacian with angular spread $10°$, but with mean angle of arrival at $45°$ (both clusters with the same power). Finally, the lower plot considers a third additional equal strength $\mathcal{L}(-45°, 10°)$ cluster. The total receive power is normalized to be the same in all three cases. Note that the beamforming gain quickly plateaus as a function of L: thus, beamforming along the dominant eigenmode captures most of the channel energy for the one cluster channel, while using the first two (three) eigenmodes captures roughly the same amount of energy in the two (three) cluster system. Thus, for typical outdoor channels, estimation of the channel covariance enables the use of a small number of eigenmodes by the demodulator and decoder, limiting complexity while preserving the SNR advantage from scaling up the number of receive elements.

The signals for L eigenmodes can be combined in a number of ways. One possibility is to explicitly estimate the scalar channels $\{\alpha_l[k]\}_{l=1}^{L}$ using pilots, and to then perform coherent diversity combining of L branches to obtain an estimate of $x[k]$. The advantage that this may have over estimation of the original $N \times 1$ channel vector $\mathbf{h}[k]$ is that fewer gains need to be explicitly estimated. In this paper, however, we consider noncoherent diversity combining, which is consistent with our goal of reducing overhead in uplink transmission. In particular, we consider the serial concatenation of an outer code with differential modulation. Joint noncoherent processing of all modes is complex. Instead, we employ a suboptimal combining strategy with iterative noncoherent processing: parallel noncoherent demodulators are employed for each mode (each employing extrinsic information from the outer decoder), the soft outputs of the demodulators are combined and sent up to the outer decoder, which then sends extrinsic information back to each of the parallel noncoherent demodulators. The details are in Section III.

III. Noncoherent Diversity Combining

We first define the block-fading channel model that is used throughout. Without loss in generality, the spatial channels are assumed to be uncorrelated with possibly unequal strengths. Thus, let $h_1, h_2, \ldots, h_L$ denote L independent Gaussian channels, with $h_l \sim \mathcal{CN}(0, \lambda_l)$, that are constant for a block of T symbols and vary independently from block to block. This model is referred to as the *parallel block fading model*. The conditional PDF of the received symbols $\mathrm{Y} = [\mathbf{y}_1\, \mathbf{y}_2\, \cdots\, \mathbf{y}_L]$ given the transmitted symbols $\mathbf{x} = [x[1]\, x[2]\, \cdots\, x[T]]^{\mathrm{T}}$ is given by

$$f_{Y|X}(\mathrm{Y}|\mathbf{x}) = \prod_{l=1}^{L} f_{Y_l|X}(\mathbf{y}_l|\mathbf{x}), \tag{4}$$

where $\mathbf{y}_l = h_l\mathbf{x} + \mathbf{n}_l$, $\mathbf{n}_l$ is AWGN with $\mathrm{E}(\mathbf{n}_j\mathbf{n}_k^{\mathrm{H}}) = 2\sigma^2\delta_{jk}\mathrm{I}_T$, and

$$f_{Y_l|X}(\mathbf{y}_l|\mathbf{x}) = \frac{\mathrm{E}\left(-\mathrm{tr}\left([2\sigma^2\mathrm{I}_T + \lambda_l\mathbf{x}\mathbf{x}^{\mathrm{H}}]^{-1}\mathbf{y}_l\mathbf{y}_l^{\mathrm{H}}\right)\right)}{\pi^T \det\left(2\sigma^2\mathrm{I}_T + \lambda_l\mathbf{x}\mathbf{x}^{\mathrm{H}}\right)} \tag{5}$$

is the conditional PDF of the Gaussian block fading channel.

The capacity is computed using ideas analogous to those of [4] for scalar channels and [11] for isotropic channels. Appendix A details the calculation for the parallel block fading channel model. Results for idealized channels, where the total power is distributed evenly amongst the top L spatial modes, are provided in [13]. The capacity notations in Figure 4 correspond to the assumptions in [13]. Figure 3(a) provides capacity results for realistic fading channels, where the top L modes are used from spatial covariance matrices generated by Laplacian PAPs and a 10-element linear array with half-wavelength spacing. The proposed transceiver performance is provided in Figures 3(b) and 4, with the details discussed next.

Given the success of iterative (or turbo) decoding techniques for approaching capacity with concatenated codes, including iterative noncoherent demodulation and decoding for the single-antenna block fading channel [4], [5], we propose a diversity combining method for parallel block fading channels

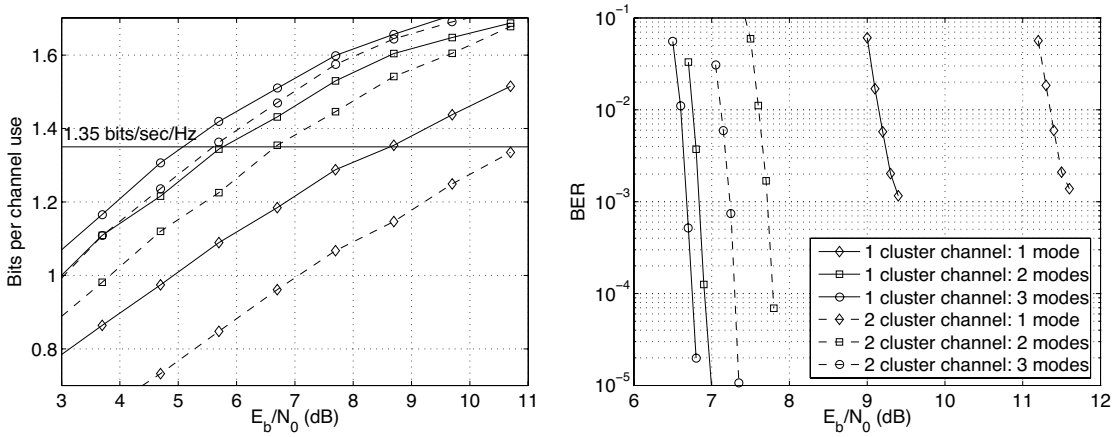

(a) Capacity of one and two cluster channels.

(b) Performance of noncoherent eigenbeamforming.

Fig. 3. Transceiver performance with multiple spatial modes for one and two cluster channels generated from Laplacian power-angle profiles.

that adheres to this architecture. Posterior probabilities (APPs) of the transmitted symbols are given by Bayes' rule,

$$P(x[k]=x|\mathrm{Y},\boldsymbol{\pi}) \propto \sum_{\mathbf{x}:x[k]=x} \prod_{t=1}^{T} P(x[t]) \prod_{l=1}^{L} f_{Y_l|X}(\mathbf{y}_l|\mathbf{x}), \tag{6}$$

where $\boldsymbol{\pi} = \{P(x[t])\}$ denotes the prior symbol probabilities. Directly implementing (6) is prohibitive, and involves joint quantization of L block fading channels, at a complexity that is Q^{L-1} times that of a single antenna system employing Q-fold quantization of the unknown channel.

We instead propose a computationally-efficient suboptimal demodulation architecture motivated by the conditional independence of the received signals $\{\mathbf{y}_l\}_{l=1}^{L}$ given the transmitted symbols $\mathbf{x}$ in (4). The approach consists of running parallel noncoherent demodulators, one for each dominant mode of the channel, and linearly combining the resulting log-domain APPs. This approach, termed noncoherent diversity combining, has the major advantage of leveraging well-known techniques for efficient noncoherent demodulation with the single antenna block fading channel [4], [5], and entails phase quantization and amplitude estimation of the unknown channel for each mode. Moreover, the complexity of noncoherent diversity combining is linear (rather than exponential) in the number of modes. Thus, we simply sum the LLRs output from each noncoherent demodulator to get an estimate of the APPs for the transmitted symbols. The decoder then computes its own posteriors for the transmitted symbols using the aggregate demodulator output, and sends them back to each demodulator for use as priors. In this fashion, joint noncoherent demodulation and decoding are performed iteratively until the codeword is decoded. Note that such diversity combining differs significantly from conventional combining of differential demodulation statistics and is able to exploit channel continuity over the coherence block.

The preceding linear diversity combining scheme is simulated with a standard rate-3/4 convolutional code, QPSK constellation, block size of $T = 10$ symbols, and codeword length of 64,000 bits. We first consider realistic fading channels and highlight the performance advantage of noncoherent eigenbeamforming transceivers when the array response is correlated. The spatial modes are generated according to outdoor channel models, as in Section II-A, with Laplacian PAPs for one and two cluster channels. As in Figure 2, the single cluster channel consists of a $\mathcal{L}(0^\circ, 10^\circ)$ PAP, and the two cluster channel is given by superposing two equal strength $\mathcal{L}(0^\circ, 10^\circ)$ and $\mathcal{L}(45^\circ, 10^\circ)$ PAPs. Capacity and performance results are given in Figure 3. The diversity combining receiver is shown to consistently operate at roughly one dB from capacity. There is significant improvement by considering two modes rather than one. The gains diminish as the number of processed modes is increased beyond three. These results demonstrate the efficiency of noncoherent eigenbeamforming receivers: the noncoherent capacity quickly plateaus as a function of the number of dominant modes considered, and the transceiver maintains near capacity performance while processing only a few modes. Thus, for outdoor channels with a few dominant modes the receiver offers complexity and performance advantages.

We next perform the following experiment: given an idealized channel in which the *total* received energy appears equally among the top L spatial modes, what is the preferred number of dominant eigen-modes for a noncoherent eigenbeamforming receiver? Figure 4 compares performance to capacity for an idealized parallel block fading channel with one, two, and three equal strength modes. The result demonstrates that near capacity performance is achieved for the one and two mode channels. For the case of a three mode channel, the transceiver exhibits a per mode noise enhancement resulting from demodulating the top modes independently. Based on this experiment, receiver performance is expected to degrade when the spatial covariance matrix is white (which is typical of indoor channels), specifically, for outdoor channels with more than two or three dominant clusters. Nevertheless, the experimental results are encouraging, since the focus is on outdoor channels with relatively few dominant modes. Further, there is a larger potential diversity gain in capacity for the two mode channel than there is by increasing the number of modes beyond two [13]. Finally, as the number of clusters grows in an outdoor environment, they are more likely to be attenuated

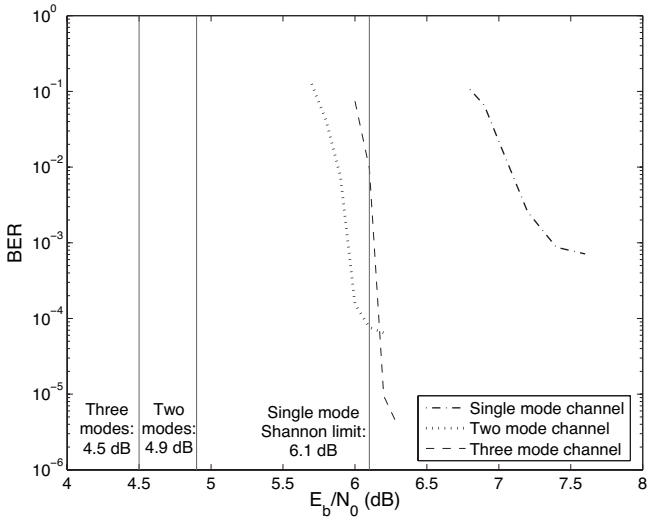

Fig. 4. Performance of noncoherent eigenbeamforming receiver at 1.35 bits/sec/Hz with idealized (where the received energy is divided equally among the given number of dominant spatial modes) parallel block fading channels, $T = 10$.

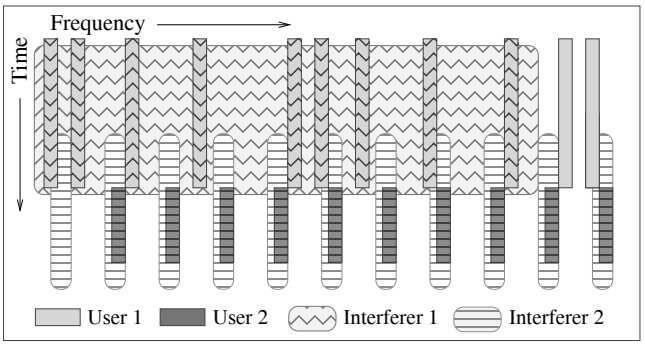

Fig. 5. Examples of spatially colored interference on the uplink of a reuse-one Orthogonal Frequency Division Multiple Access (OFDMA) system. User 1 is interfered by a wideband signal with similar spatial modes at the base station. User 2 is interfered by an edge user from an adjacent cell employing a similar resource assignment.

from the dominant cluster (contributing most of the received energy), which would serve to mitigate the noise enhancement effect.

IV. Interference Suppression

Interference from neighboring cells in OFDM systems with high spatial reuse is largely mitigated by random-like scheduling in time and frequency. Inter-cell interference is further avoided in synchronous systems via coordinated Time Division Multiplexing (TDM) and Frequency Division Multiplexing (FDM) scheduling and power control techniques. Estimates of the desired user's spatial covariance matrix,

$$\mathrm{C_S} = \mathrm{E}(\mathbf{a}(\Omega_\mathrm{S})\mathbf{a}(\Omega_\mathrm{S})^\mathrm{H}), \tag{7}$$

rely on averaging over many subcarriers. If the interference in different subcarriers is spatially uncorrelated, then their contribution to the overall spatial covariance matrix is approximately white. Thus, uplink averaging provides a good estimate of the spatial modes of the desired signal. However, if the uplink schedule of a radio in the nearby cell overlaps significantly with that of the desired user, as depicted in Figure 5, then the resulting interference is spatially colored and can contribute significantly to the dominant spatial eigenmodes in the received signal. In this case, the preceding estimate of the spatial covariance matrix is insufficient to distinguish the spatial modes of the desired signal and interference. We show that using a small number of pilot symbols in the transmitted signal (much smaller than what would be required for coherent reception) it is possible to extract the modes for the desired signal while suppressing the colored interference.

Our approach for dealing with colored spatial interference is summarized as follows: (a) project down to the signal subspace corresponding to the dominant eigenmodes, (b) compute linear MMSE type interference-suppressing correlators using pilot symbols for a selected number of subcarriers, and (c) find a single interference-suppressing correlator that works well over the entire frequency band, exploiting the fact that the signal and interference spatial modes are the same across frequency. The projection step (a) reduces the dimension of the interference-suppressing correlator, and reduces the number of pilot symbols needed in step (b).

The specific mechanism that we use for adaptation is based on a variation of the Differential MMSE (DMMSE) criterion, developed for direct sequence CDMA systems with multipath fading channels in [6]. DMMSE-based adaptation is robust to time variations, and leads to a bank of spatial correlators which extract energy from the desired signal while suppressing the interference.

A. Interference model

We consider the case of zero dB interference $\{x_\mathrm{I}[k]\}$ that is uncorrelated with the desired signal $\{x_\mathrm{S}[k]\}$. This in particular means that the signal and interference have the same energy, which is normalized to one: $\mathrm{E}(|x_\mathrm{S}[k]|^2) = \mathrm{E}(|x_\mathrm{I}[k]|^2) = 1$. Analogous to the signal model (7), the $N \times 1$ interference channel is modeled as Gaussian with zero-mean and covariance $\mathrm{C_I} = \mathrm{E}(\mathbf{a}(\Omega_\mathrm{I})\mathbf{a}(\Omega_\mathrm{I})^\mathrm{H})$. The array response $\mathbf{a}(\Omega_\mathrm{I})$ varies according to the PAP of the interference angle of arrival, Ω_I. The PAPs of the interference and data channels are modeled as independent Laplacians, with the same variance but differing mean angles of arrival. This corresponds to a scenario in which the interference process is virtually indistinguishable from an additional mode of the desired signal when detected noncoherently.

The baseband received symbol vector at subcarrier k is then

$$\mathbf{y}[k] = \mathbf{h}_\mathrm{S}[k]x_\mathrm{S}[k] + \mathbf{h}_\mathrm{I}[k]x_\mathrm{I}[k] + \mathbf{n}[k],$$

with $\mathbf{h}_\mathrm{S}[k] \sim \mathcal{CN}(0, \mathrm{C_S})$, $\mathbf{h}_\mathrm{I}[k] \sim \mathcal{CN}(0, \mathrm{C_I})$, and $\mathbf{n}[k] \sim \mathcal{CN}(0, 2\sigma^2\mathrm{I}_N)$. Letting $\mathrm{V} = [\mathbf{v}_1, \ldots, \mathbf{v}_L]$ denote the dominant eigenvectors of $\mathrm{E}(\mathbf{y}[k]\mathbf{y}[k]^\mathrm{H})$, eigenbeamforming consists of projecting the received signal down to the reduced ($L \ll N$) subspace spanned by the columns of V. This yields the following sufficient statistic for the transmitted symbol sequence:

$$\mathbf{z}[k] = \mathrm{V}^\mathrm{H}\mathbf{y}[k] = \boldsymbol{\alpha}_\mathrm{S}[k]x_\mathrm{S}[k] + \boldsymbol{\alpha}_\mathrm{I}[k]x_\mathrm{I}[k] + \mathbf{w}[k], \tag{8}$$

with $\boldsymbol{\alpha}_\mathrm{S}[k] \sim \mathcal{CN}(0, \Sigma_\mathrm{S})$, $\boldsymbol{\alpha}_\mathrm{I}[k] \sim \mathcal{CN}(0, \Sigma_\mathrm{I})$, and $\mathbf{w}[k] \sim \mathcal{CN}(0, 2\sigma^2\mathrm{I}_L)$. Where $\Sigma_\mathrm{S} = \mathrm{V}^\mathrm{H}\mathrm{C_S}\mathrm{V}$ and $\Sigma_\mathrm{I} = \mathrm{V}^\mathrm{H}\mathrm{C_I}\mathrm{V}$ are defined to be the signal and interference covariance in the

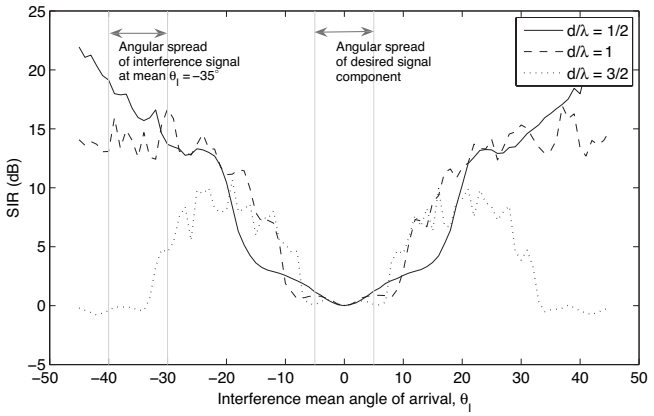

Fig. 6. Signal-to-Interference Ratio (SIR) of ideal MMSE interference suppression with a 10 element linear receive array.

reduced-space. The spatial covariance matrix of the received signal, (8), is thus given by

$$\mathrm{R} = \mathrm{E}\left(\mathbf{z}[k]\mathbf{z}[k]^{\mathrm{H}}\right) = \Sigma_{\mathrm{S}} + \Sigma_{\mathrm{I}} + 2\sigma^2\mathrm{I}_L.$$

B. MMSE framework

As an unrealizable benchmark, we first discuss an ideal MMSE receiver for the received signal model (8), which has access to the data and interference spatial channel realizations.

The MMSE criterion [20], [21] is defined as

$$\mathbf{c} = \arg\min \mathrm{E}(|\langle \mathbf{c}, \mathbf{z}[k]\rangle - x_{\mathrm{S}}[k]|^2). \tag{9}$$

The well known least squares solution is given by $\mathbf{c} = \mathrm{R}^{-1}\mathbf{p}$, where $\mathbf{p} = \mathrm{E}(x_{\mathrm{S}}^*[k]\mathbf{z}[k])$. Substituting channel realizations for statistical expectations yields the ideal MMSE filter:

$$\mathbf{c}_{\text{ideal}}[k] = (\boldsymbol{\alpha}_{\mathrm{S}}[k]\boldsymbol{\alpha}_{\mathrm{S}}[k]^{\mathrm{H}} + \boldsymbol{\alpha}_{\mathrm{I}}[k]\boldsymbol{\alpha}_{\mathrm{I}}[k]^{\mathrm{H}} + 2\sigma^2\mathrm{I}_L)^{-1}\boldsymbol{\alpha}_{\mathrm{S}}[k]. \tag{10}$$

As a measure of the performance of ideal MMSE interference suppression, we evaluate the Signal-to-Interference Ratio (SIR) at the correlator output, defined as,

$$\frac{\mathrm{E}\left(|\langle \mathbf{c}_{\text{ideal}}[k], \boldsymbol{\alpha}_{\mathrm{S}}[k]\rangle|^2\right)}{\mathrm{E}\left(|\langle \mathbf{c}_{\text{ideal}}[k], \boldsymbol{\alpha}_{\mathrm{I}}[k]\rangle|^2\right)}.$$

For this purpose, the signal and interference PAPs are modeled as Laplacian, $\mathcal{L}(\cdot, \Delta)$, with means θ_{S} and θ_{I}, respectively, and a common angular spread of $\Delta = 10°$. Figure 6 displays MMSE SIR as a function of the mean angle of arrival of the interference PAP, where the PAP of the desired signal is taken to be zero-mean. This Figure shows, for example, that half-wavelength spaced antenna arrays are in principle better able to resolve interference at mean angles of arrival between 30 and 45 degrees.

For continuously fading channels, the ideal MMSE solution must be calculated separately for each coherence block, since the spatial channel realizations vary significantly across subcarriers. On the other hand, the spatial covariances for both the desired signal and the colored interference (Σ_{S} and Σ_{I}, respectively), averaged across subcarriers, vary more slowly across time. Thus, in the following, interference suppressing correlators that can be used across subcarriers are computed using the DMMSE criterion.

Noncoherent demodulation and decoding is then performed as previously described, after applying these spatial correlators. The amount of pilot overhead required for computing the correlators is about 2%, which is far less than the overhead required for tracking channel realizations on a per-subcarrier basis.

C. The DMMSE correlator

We refer to [6] for a detailed development of the DMMSE criterion, where it is assumed that the channel can be approximated as constant over two consecutive symbols. In this section, we generalize the criterion in [6] to apply to coherence blocks of arbitrary size. We summarize the key concepts here and adapt the DMMSE criterion for our purpose.

First, note that standard MMSE adaptation fails over Rayleigh fading channels essentially because the estimate of the desired signal vector averages to zero over a long enough adaptation interval: $\mathbf{p} = \mathrm{E}(\boldsymbol{\alpha}_{\mathrm{S}})\,\mathrm{E}(|x_{\mathrm{S}}[k]|^2) = 0$. Next, we make the following observation: if a correlator suppresses interference, then over a coherence block, its output satisfies:

$$\langle \mathbf{c}, \mathbf{z}[k]\rangle \approx \beta x_{\mathrm{S}}[k], \quad k \in \mathcal{T} \tag{11}$$

where β is an arbitrary complex scalar. Note that, as long as β is nonzero, the output of the correlator is amenable to block noncoherent demodulation.

The symbols $x_{\mathrm{S}}[k]$ are known for a certain number of coherence blocks containing pilot symbols, say $\mathcal{T}_1, ..., \mathcal{T}_P$. We can now try to enforce (11) for these pilot blocks by minimizing the sum of $\sum_{k\in\mathcal{T}} |\langle \mathbf{c}, \mathbf{z}[k]\rangle - \beta x_{\mathrm{S}}[k]|^2$ over these blocks. Note that the unknown complex scalar β can be different from block to block, and can be arbitrary (as long as it is nonzero). It therefore makes sense to minimize over both $\mathbf{c}$ and β. This leads to the following adaptation criterion: minimize

$$J(\mathbf{c}) = \sum_{i=1}^{P} \min_{\beta_i} \sum_{k\in\mathcal{T}_i} |\langle \mathbf{c}, \mathbf{z}[k]\rangle - \beta_i x_{\mathrm{S}}[k]|^2. \tag{12}$$

The solution to the preceding problem is $\mathbf{c} = 0$ and $\beta_i = 0$ for $i = 1, ..., P$. To avoid this trivial solution, we impose the constraint on the energy at the output of the correlator:

$$\mathrm{E}\left(|\langle \mathbf{c}, \mathbf{z}[k]\rangle|^2\right) = \mathbf{c}^{\mathrm{H}}\mathbf{R}\mathbf{c} = 1. \tag{13}$$

We therefore obtain the following adaptation criterion.

DMMSE adaptation criterion: Minimize $J(\mathbf{c})$ subject to the constraint (13).

We now derive the solution to the preceding optimization problem. The first step is the solution to the inner minimization problem, in order to compute

$$J_i(\mathbf{c}) = \min_{\beta_i} \sum_{k\in\mathcal{T}_i} |\langle \mathbf{c}, \mathbf{z}[k]\rangle - \beta_i x_{\mathrm{S}}[k]|^2$$

Since the function to be minimized is quadratic in β_i, it is straightforward to show by differentiation that the minimum value is

$$J_i(\mathbf{c}) = \left(\sum_{k\in\mathcal{T}_i} |\langle \mathbf{c}, \mathbf{z}[k]\rangle|^2\right) - E_i\mathbf{c}^{\mathrm{H}}\mathbf{p}_i\mathbf{p}_i^{\mathrm{H}}\mathbf{c} \tag{14}$$

where

$$E_i = \sum_{k \in \mathcal{T}_i} |x_{\mathrm{S}}[k]|^2 \tag{15}$$

and

$$\mathbf{p}_i = \frac{\sum_{k \in \mathcal{T}_i} x_{\mathrm{S}}^*[k]\mathbf{z}[k]}{\sum_{k \in \mathcal{T}_i} |x_{\mathrm{S}}[k]|^2} \tag{16}$$

The vector $\mathbf{p}_i$ is an estimate of the spatial channel of the desired user over the coherence block $\mathcal{T}_i$.

The function to be minimized is therefore

$$J(\mathbf{c}) = \sum_{i=1}^{P} J_i(\mathbf{c}) = \left(\sum_{i=1}^{P} \sum_{k \in \mathcal{T}_i} |\langle \mathbf{c}, \mathbf{z}[k] \rangle|^2 \right) - \sum_{i=1}^{P} E_i \mathbf{c}^{\mathrm{H}} \mathbf{p}_i \mathbf{p}_i^{\mathrm{H}} \mathbf{c}$$

The first term on the right hand side is simply the empirical output energy, which must be held roughly constant by virtue of the constraint (13). We can therefore ignore this term and obtain the following equivalent optimization problem. For simplicity of notation, we assume a constant modulus constellation (at least for the pilot symbols), setting $|x_{\mathrm{S}}[k]|^2 = 1$. In this case, if a coherence block contains T symbols, then $E_i = T$ for all i, and we have

$$\mathbf{p}_i = \frac{1}{T} \sum_{k \in \mathcal{T}_i} x_{\mathrm{S}}^*[k]\mathbf{z}[k].$$

Reduced optimization problem: Maximize $\mathbf{c}^{\mathrm{H}} \hat{\mathrm{A}} \mathbf{c}$ subject to $\mathbf{c}^{\mathrm{H}} \hat{\mathrm{R}} \mathbf{c} = 1$, where

$$\hat{\mathrm{A}} = \frac{1}{P} \sum_{i=1}^{P} \mathbf{p}_i \mathbf{p}_i^{\mathrm{H}}$$

and $\hat{\mathrm{R}}$ is an estimate of the spatial covariance, given by

$$\hat{\mathrm{R}} = \frac{1}{K} \sum_{k=1}^{K} \mathbf{z}[k]\mathbf{z}[k]^{\mathrm{H}}$$

Note that $\hat{\mathrm{R}}$ can be computed by averaging over all symbols, not just TP pilot symbols.

It is easy to see by differentiating the Lagrangian for the preceding optimization problem that the solution must satisfy the following generalized eigenvalue equation:

$$\hat{\mathrm{A}} \mathbf{c} = \lambda \hat{\mathrm{R}} \mathbf{c}. \tag{17}$$

Combining (13) and (17) yields $\lambda = \mathbf{c}^{\mathrm{H}} \hat{\mathrm{A}} \mathbf{c}$. As λ is the quantity to be maximized, DMMSE correlators are given by the dominant eigenvectors of $\hat{\mathrm{R}}^{-1} \hat{\mathrm{A}}$.

The cost function $J(\mathbf{c})$ in (12) can now be written as

$$J(\mathbf{c}) = TP \mathbf{c}^{\mathrm{H}} (\hat{\mathrm{R}} - \hat{\mathrm{A}}) \mathbf{c}.$$

In order for this to be approximately zero, we must have $\lambda \approx 1$. Thus, for channels with multiple dominant modes, the correlators with eigenvalues near one can be selected for demodulation. Similar to the criterion developed in [6], simulations have shown that selecting the correlators based on $\lambda > 0.5$ yields good performance.

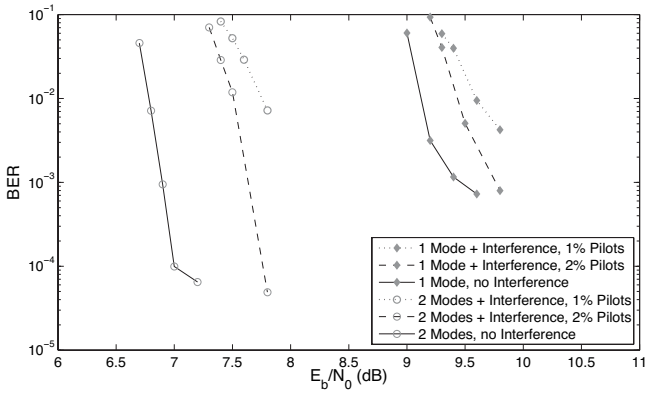

Fig. 7. Performance of DMMSE based interference suppression with zero dB interference separated by 45 degrees.

D. Numerical results

The model in (8) is employed for simulation of a coded system. The signal and interference spatial covariance matrices are computed based on Laplacian PAPs and a 10-element half-wavelength spaced linear array. In particular, the signal and interference angles of arrival, Ω_{S} and Ω_{I}, are distributed as $\Omega_{\mathrm{S}} \sim \mathcal{L}(0^\circ, 10^\circ)$ and $\Omega_{\mathrm{I}} \sim \mathcal{L}(45^\circ, 10^\circ)$. These PAPs model single cluster data and interference channels, characterized by one or two dominant spatial modes. Correlators based on the DMMSE criterion (17) are employed to suppress the zero dB interference process.

Figure 7 compares the performance of convolutional coded differential QPSK modulation at rate-1.35 bits/symbol with no interference to DMMSE suppression of the interference process. The codeword length is chosen to be 64,000 bits, and the coherence length of the channel is $T = 10$ symbols. The spatial modes of the signal and interference channels are assumed to be static over the transmitted codeword. The channel modes are estimated based on pilot symbols, a certain fraction of the overall transmitted symbols, that are sent in bursts matching the coherence block size. Performance of DMMSE interference suppression is within 0.5 dB of the performance without interference. Approximately 0.1 dB of this gap is attributed to the 2% pilot overhead. Given the performance improvement for diversity combining with the top two modes of a one cluster channel with no interference, we employ the top two DMMSE correlators for diversity combining in the presence of interference. The results are also shown in Figure 7, demonstrating comparable performance to eigenbeamforming with $L = 2$ and no interference.

V. Conclusions

We have proposed a new receiver architecture for OFDM-based uplinks for outdoor mobile communication. The key idea is to exploit the small number of spatial modes in such channels to obtain large performance gains by scaling up the number of base station antennas, without incurring a corresponding increase in receiver complexity. Our results show that overhead-free methods can be used to obtain beamforming, and in certain cases even diversity gains, without explicit estimation of channel realization, thus dramatically reducing or eliminating pilot overhead for channel tracking.

Noncoherent demodulation and decoding strategies are effective in approaching information-theoretic benchmarks for channels approximated with a block fading model. For strong, spatially colored interference, we show the effectiveness of pilot-based adaptive interference suppression techniques, consistent with block noncoherent demodulation and decoding and based on the DMMSE criterion. The amount of pilot overhead for DMMSE training is far less than required for coherent techniques. We observe that it is possible to suppress interference of strength equal to that of the desired user, as long as the spatial responses are sufficiently separable. The case of one antenna at the mobile is treated for representational simplicity and serves to highlight the concept of noncoherent eigenbeamforming. In practice the mobile may have one or more antennas, and the proposed transceiver is readily generalized, depending on the amount of feedback assumed. For example, multiple transmit antennas can be used to implement diversity/switching techniques, transmit beamforming techniques, or certain space-time techniques such as noncoherent Alamouti code [22].

While our results demonstrate the feasibility of beamforming and interference suppression gains without requiring a traditional coherent architecture, more detailed design and performance evaluation under a number of channel models, and accounting for medium access control protocols, are needed for evaluating a noncoherent uplink architecture. An important practical consequence of our results is that the base station antennas for outdoor applications should be spaced relatively close together (e.g., less than half the wavelength) in order to optimize for beamforming and interference suppression rather than for spatial diversity. A similar observation holds for the (coherent) downlink architecture proposed in [1]. Our results also provide guidelines for spatial reuse: based on the spatial interference suppression capability of the architecture, we can say, for example, that simultaneous reception from two different sectors of the same cell appears to be feasible, as long as the users are about 30-45 degrees apart.

APPENDIX A
CAPACITY OF PARALLEL BLOCK FADING CHANNELS

Computational techniques employed here are analogous to those used in [4] for the case of scalar block fading channels and [11] for isotropic channels. The capacity of parallel block fading channels (4)-(5) is given by:

$$\mathcal{C} = \sup I(\mathrm{Y};\mathbf{x}) = \sup\{H(\mathrm{Y}) - H(\mathrm{Y}|\mathbf{x})\}, \qquad (18)$$

over space of input alphabets $(\mathcal{X}, P(\mathbf{x}))$, satisfying the average power constraint $\mathrm{E}[\|\mathbf{x}\|^2] = T$. First, entropy of the received signal is computed as $H(\mathrm{Y}) = -\,\mathrm{E}\log f_{Y|X}(\mathrm{Y}|\mathbf{1})$, where $\mathbf{1}$ denotes the all ones vector, with Monte-Carlo integration over the space of $\mathbf{h}$ and N. The conditional entropy term, $H(\mathrm{Y}|\mathbf{x})$, is then evaluated in closed form.

Definition 1: The MPSK signal vector $\mathbf{x} \in \mathcal{X}$ is written as a unitary matrix times the all ones vector $\mathbf{x} = \Phi(\mathbf{x})\mathbf{1}$, where $\Phi(\mathbf{x}) = \mathrm{diag}(x_1, x_2, ..., x_T)$. We refer to Φ of this form as a "discrete rotation," since, $\mathcal{X} = \Phi\mathcal{X}$, the signal alphabet is the same with all of its elements rotated by Φ.

The following lemma implies that the PDF of Y is invariant to discrete rotations.

Lemma 1: Let U denote a unitary matrix, then $f_{Y|X}(\mathrm{UY}|\mathbf{x}) = f_{Y|X}(\mathrm{Y}|\mathrm{U}^{\mathrm{H}}\mathbf{x})$.

Proof: Letting f_N denote the noise density function,

$$\begin{aligned} f_{Y|X}(\mathrm{UY}|\mathbf{x}) &= \prod_{l=1}^{L} f_{Y_l|X}(\mathrm{U}\mathbf{y}_l|\mathbf{x}) \\ &= \prod_{l=1}^{L} \mathrm{E}(f_N(\mathrm{U}\mathbf{y}_l - \sqrt{\lambda_l}h\mathbf{x})) \\ &= \prod_{l=1}^{L} \mathrm{E}(f_N(\mathbf{y}_l - \sqrt{\lambda_l}h\mathrm{U}^{\mathrm{H}}\mathbf{x})) \\ &= f_{Y|X}(\mathrm{Y}|\mathrm{U}^{\mathrm{H}}\mathbf{x}), \end{aligned}$$

where expectations are taken with respect to a Gaussian $\mathcal{CN}(0,1)$ distributed fading coefficient h, and the third equality follows from circular symmetry of complex Gaussian PDF. ■

Corollary 1: For any discrete rotation, Φ, $f_Y(\Phi\mathrm{Y}) = f_Y(\mathrm{Y})$.

Proof: Given the above Lemma, we have

$$\begin{aligned} f_Y(\Phi\mathrm{Y}) &= \frac{1}{M^T}\sum_{\mathbf{x}\in\mathcal{X}} f_{Y|X}(\Phi\mathrm{Y}|\mathbf{x}) \\ &= \frac{1}{M^T}\sum_{\mathbf{x}\in\mathcal{X}} f_{Y|X}(\mathrm{Y}|\Phi^{\mathrm{H}}\mathbf{x}) \\ &= \frac{1}{M^T}\sum_{\mathbf{x}\in\Phi^{\mathrm{H}}\mathcal{X}} f_{Y|X}(\mathrm{Y}|\mathbf{x}) \\ &= f_Y(\mathrm{Y}) \end{aligned}$$

■

Proposition 1: $H(\mathrm{Y}) = -\,\mathrm{E}\,(\log f_Y(\mathrm{Y})|\mathbf{x} = \mathbf{1})$

Proof:

$$\begin{aligned} H(\mathrm{Y}) &= -\int d\mathrm{Y} f_Y(\mathrm{Y})\log f_Y(\mathrm{Y}) \\ &= -\frac{1}{M^T}\int d\mathrm{Y}\sum_{\mathbf{x}\in\mathcal{X}} f_{Y|X}(\mathrm{Y}|\mathbf{x})\log f_Y(\mathrm{Y}) \\ &= -\frac{1}{M^T}\sum_{\mathbf{x}\in\mathcal{X}}\int d\mathrm{Y} f_{Y|X}(\Phi(\mathbf{x})^{\mathrm{H}}\mathrm{Y}|\mathbf{1})\log f_Y(\mathrm{Y}) \\ &= -\frac{1}{M^T}\sum_{\mathbf{x}\in\mathcal{X}}\int d\mathrm{Y} f_{Y|X}(\mathrm{Y}|\mathbf{1})\log f_Y(\Phi(\mathbf{x})\mathrm{Y}) \\ &= -\int d\mathrm{Y} f_{Y|X}(\mathrm{Y}|\mathbf{1})\log f_Y(\mathrm{Y}) \\ &= -\,\mathrm{E}(\log f_Y(\mathrm{Y})|\mathbf{x} = \mathbf{1}), \end{aligned}$$

since the Jacobian determinant of a unitary matrix is one. ■

For the conditional entropy of Y given $\mathbf{x}$: conditioned on $\mathbf{x}$, $\{\mathbf{y}_l\}$ are independent Gaussian random vectors with entropy $H(\mathbf{y}_l|\mathbf{x}) = \log\det(\pi e\,\mathrm{E}(\mathbf{y}_l\mathbf{y}_l^{\mathrm{H}}))$. Then,

$$H(\mathrm{Y}|\mathbf{x}) = \sum_{l=1}^{L} H(\mathbf{y}_l|\mathbf{x}) = LT\log(2\pi e\sigma^2) + \log\Big(\prod_{l=1}^{L}(1+\frac{\lambda_l T}{2\sigma^2})\Big).$$

REFERENCES

[1] G. Barriac and U. Madhow, "Space-time communication for OFDM with implicit channel feedback," *IEEE Trans. Inform. Theory*, vol. 50, no. 12, pp. 3111–3129, Dec. 2004.

[2] ——, "Characterizing outage rates for space-time communication over wideband channels," *IEEE Trans. Commun.*, vol. 52, no. 12, pp. 2198–2208, Dec. 2004.

[3] M. Peleg, S. Shamai, and S. Galán, "Iterative decoding for coded noncoherent MPSK communications over phase-noisy AWGN channel," *IEE Proc. Commun.*, vol. 147, no. 2, pp. 87–95, Apr. 2000.

[4] R.-R. Chen, R. Koetter, D. Agrawal, and U. Madhow, "Joint demodulation and decoding for the noncoherent block fading channel: a practical framework for approaching channel capacity," *IEEE Trans. Commun.*, vol. 51, no. 10, pp. 1676–1689, Oct. 2003.

[5] N. Jacobsen and U. Madhow, "Reduced-complexity noncoherent communication with differential QAM and iterative receiver processing," in *Proc. Conf. on Information Sciences and Systems (CISS)*, Baltimore, MD, USA, Mar. 2003.

[6] U. Madhow, K. Bruvold, and Z. Liping, "Differential MMSE: a framework for robust adaptive interference suppression for DS-CDMA over fading channels," *IEEE Trans. Commun.*, vol. 53, no. 8, pp. 1377–1390, Aug. 2005.

[7] E. Telatar, "Capacity of multi-antenna Gaussian channels," *European Trans. Telecomm.*, vol. 10, no. 6, pp. 585–596, Nov. 1999.

[8] S. M. Alamouti, "A simple transmit diversity technique for wireless communications," *IEEE J. Select. Areas Commun.*, vol. 16, no. 8, p. 14511458, Oct. 1998.

[9] V. Tarokh, N. Seshadri, and A. R. Calderbank, "Space-time codes for high data rate wireless communication: Performance analysis and code construction," *IEEE Trans. Inform. Theory*, vol. 44, no. 2, p. 744765, Mar. 1998.

[10] G. Golden, G. J. Foschini, R. A. Valenzuela, and P. W. Wolniansky, "V-BLAST: a high capacity space-time architecture for the rich-scattering wireless channel," in *Proc. Fifth Workshop on Smart Antennas in Wireless Mobile Communications*, Stanford Univ., CA, USA, July 1998.

[11] T. L. Marzetta and B. M. Hochwald, "Capacity of a mobile multiple-antenna communication link in Rayleigh flat fading," *IEEE Trans. Inform. Theory*, vol. 45, no. 1, pp. 139–157, Jan. 1999.

[12] L. Zheng and D. Tse, "Communicating on the Grassmann manifold: A geometric approach to the non-coherent multiple antenna channel," *IEEE Trans. Inform. Theory*, vol. 48, no. 2, pp. 359–383, Feb. 2002.

[13] N. Jacobsen, G. Barriac, and U. Madhow, "Noncoherent eigenbeamforming for a wideband cellular uplink," in *Proc. IEEE International Symp. on Information Theory (ISIT)*, Chicago, IL, USA, June 2004.

[14] A. Steiner, M. Peleg, and S. Shamai, "Iterative decoding of space-time differentially coded unitary matrix modulation," *IEEE Trans. Signal Processing*, vol. 50, no. 10, pp. 2383–2395, Oct. 2002.

[15] M. K. Varanasi, "A systematic approach to the design and analysis of optimum DPSK receivers for generalized diversity communications over rayleigh fading channels," *IEEE Trans. Commun.*, vol. 47, no. 9, pp. 1365–1375, Sept. 1999.

[16] D. Gesbert, M. Shafi, S. Da-shan, P. Smith, and A. Naguib, "From theory to practice: an overview of MIMO space-time coded wireless systems," *IEEE J. Select. Areas Commun.*, vol. 21, no. 3, pp. 281–302, Apr. 2003.

[17] G. Barriac and U. Madhow, "Wideband space-time communication with implicit channel feedback," in *Proc. Seventh International Symp. on Signal Processing and its Applications*, July 2003.

[18] A. Saleh and R. Valenzuela, "A statistical model for indoor multi-path propagation," *IEEE J. Select. Areas Commun.*, vol. 5, no. 2, pp. 128–137, Feb. 1987.

[19] K. I. Pedersen, P. E. Mogensen, and B. H. Fleury, "Dual-polarized model of outdoor propagation environments for adaptive antennas," in *Proc. IEEE 49th Vehicular Technology Conference*, vol. 2, May 1999, pp. 990–995.

[20] H. V. Poor, *An Introduction to Signal Detection and Estimation*. Springer-Verlag, 1994.

[21] U. Madhow and M. L. Honig, "MMSE interference suppression for direct-sequence spread-spectrum CDMA," *IEEE Trans. Commun.*, vol. 42, no. 12, pp. 3178–3188, Dec. 1994.

[22] M. L. B. Riediger and P. K. M. Ho, "An eigen-assisted noncoherent receiver for Alamouti-type space-time modulation," *IEEE J. Select. Areas Commun.*, vol. 23, no. 9, pp. 1811–1820, Sept. 2005.

Noah Jacobsen received the B.S. degree in electrical engineering from Cornell University, Ithaca, NY in 2000, and the M.S. and Ph.D. degrees in electrical engineering from the University of California, Santa Barbara in 2005. He is currently with Alcatel-Lucent, Murray Hill, NJ.

Gwen Barriac received the B.S. degree in electrical engineering from Princeton University, Princeton, NJ, in 1999, and the M.S. and Ph.D. degrees in electrical engineering from the University of California at Santa Barbara in 2004. She is currently with Qualcomm, San Diego, CA.

Upamanyu Madhow is a Professor of Electrical and Computer Engineering at the University of California, Santa Barbara. His research interests are in communication systems and networking, with current emphasis on wireless communication, sensor networks and multimedia security.

He received his bachelor's degree in electrical engineering from the Indian Institute of Technology, Kanpur, in 1985, and his Ph. D. degree in electrical engineering from the University of Illinois, Urbana-Champaign in 1990. He has worked as a research scientist at Bell Communications Research, Morristown, NJ, and as a faculty at the University of Illinois, Urbana-Champaign.

Dr. Madhow is a recipient of the NSF CAREER award. He has served as Associate Editor for Spread Spectrum for the *IEEE Transactions on Communications*, and as Associate Editor for Detection and Estimation for the *IEEE Transactions on Information Theory*. He currently serves as Associate Editor for the *IEEE Transactions on Information Forensics and Security*. He is the author of the textbook *Fundamentals of Digital Communication,* published by Cambridge University Press in 2008.